A quality by design approach for the synthesis of palmitoyl carnitine loaded nanoemulsions as drug delivery systems.

Eva Arroyo-Urea[1], María Muñoz-Hernando[1], Marta Leo-Barriga[1], Fernando Herranz[1,2,3],* Ana González-Paredes[1,3]*

[1]Nanomedicine and Molecular Imaging group, Instituto de Química Médica-CSIC, Juan de la Cierva, 3- 28006 Madrid (Spain)
[2]Centro de Investigación Biomédica en Red de Enfermedades Respiratorias (CIBERES)
[3]Conexión Nanomedicina-CSIC

**Corresponding authors:* ana.gonzalez@iqm.csic.es, fherranz@iqm.csic.es

ABSTRACT
Hypothesis:
Nanoemulsions (NE) are lipid nanocarriers that can efficiently load hydrophobic active compounds, like palmitoyl-L-carnitine (pC), used here as model molecule. The use of design of experiments (DoE) approach is a useful tool to develop NE with optimized properties, requiring less experiments compared to trial-and-error approach. The optimized formulation was studied for its stability, scalability, pC entrapment, loading capacity, and biodistribution in mice.
Experiments:
NE were prepared by the solvent injection technique. DoE was implemented for designing pC-loaded NE, using a two-level fractional factorial design as model. NE were fully characterized by a combination of techniques, and biodistribution was studied *ex-vivo* after injection of fluorescent NE in healthy mice.
Findings:
We selected the optimal formulation of NE, named pC-NE_U, after DoE analysis of four variables. pC-NE_U incorporated pC in a very efficient manner, with high entrapment efficiency and loading capacity. pC-NE_U did not change its initial colloidal properties stored at 4ºC in water during 120 days, nor in buffers with different pH values (5.3 and 7.4) during 30 days. The scalability process did not affect NE stability properties. Biodistribution study showed that pC-NE_U formulation was predominantly concentrated in the liver, with minimal accumulation in spleen, stomach and kidneys.

Keywords:
Nanoemulsion, drug delivery, design of experiments, colloidal stability, biodistribution

1. INTRODUCTION

Drug delivery nanosystems are designed technologies that allow drugs to be transported in a controlled manner. Because of their usefulness in modulating drug release, protecting labile materials (e.g., peptides, DNA or mRNA) against degradation, and site-specific drug targeting, a lot of research is going into producing nanoparticles as drug vehicles, especially now with the new generation of lipid nanoparticle-based vaccines [1,2].

According to the different materials used to construct the carrier, nanoplatforms can be roughly divided in two types: inorganic and organic nanosystems, belonging to the last one the lipid-based and polymeric-based nanocarriers, among others [3]. Advantages of both systems include a good profile of controlled release, excellent physical stability, or an easy scalability [4,5]. However, the low encapsulation rate of polymer nanoparticles and the use of huge amounts of organic solvents in their production process is making lipid-based nanoparticles to receive more attention [6]. In fact, because of their

biocompatibility and formulation simplicity, across the pharmaceutical industry they are considered as the most promising vehicles to deliver a variety of therapeutics [7].

We can distinguish four main categories among lipid-based nanoplatforms: liposomes, nanoemulsions (NE, made of liquid lipids), solid lipid nanoparticles (made of solid lipids), and nanostructured lipid carriers (made of mixtures of solid and liquid lipids) [8]. Compared to other nanocarriers, nanoemulsions are gaining increasingly interest for drug delivery due to their simple composition and easy production. Nanoemulsions are generally constituted by oil, water and a surfactant, with droplet sizes ranging from 10 to 1000 nm. According to their structure, NE can be classified in three types: oil in water (O/W), water in oil (W/O), and bi-continuous/multiple emulsion where micro domains of oil and water phases are inter-dispersed (W/O/W and O/W/O) [9,10].

Among the advantages of using NE we can highlight the improvement of the bioavailability of hydrophobic drugs [11]. Considerable research is nowadays ongoing to encapsulate hydrophobic drugs for improved bioavailability, safety, and efficacy [12–15]. Nevertheless, developing a versatile and controllable drug encapsulation system with high drug loading still remains a challenge. For the various nanoparticle systems reported, drug loading is usually below 10 % or even 1 % [16]. Due to their recognized ability for facilitating the encapsulation of the hydrophobic molecules through the lipid matrix, NE have been used to wrap essential oils and nutrients, and a large number of studies have reported using them to package different types of drugs such as paclitaxel [17], curcumin [18] and retinoic acid [19], among others.

In recent years pharmaceutical industry is implementing Quality by Design (QbD) approaches motivated by the stringent need of ensure and enhance products safety, quality and efficacy [20]. Considering QbD, product quality can be controlled by the identification of critical factors —independent variables— and their influence in obtained responses —dependent variables— allowing the optimization of the process. The QbD approach involves statistical design of experiments (DoE) which allows to identify the relationships between the factors influencing a process and the observed outputs, and helping in the identification of optimal process conditions within the space of the design [21]. Compared to trial-and-error and one-factor-at-time (OFAT) approaches, DoE provides more information from datasets, allowing minimization of experimental efforts for a given statistical power and giving the possibility of working with different type of constrains [22]. Furthermore, a thorough understanding of these processes is essential for later scale-up and quality control as needed for preclinical and clinical test batches. Although DoE has several advantages in the rational design of lipid nanoparticles, its use is still scarce in the literature. Nevertheless, the most frequently evaluated responses are particle size, polydispersity index (PDI), zeta potential, drug loading and entrapment efficiency, as these are parameters that highly influence particles stability and biological behavior, whereas the studied factors influencing these responses are related to lipids and surfactants composition and conditions for synthesis [23].

Our aim was to use QbD approach to develop a O/W nanoemulsion with optimal physico-chemical and colloidal stability properties as drug carrier for encapsulation of hydrophobic drugs, using palmitoyl-L-carnitine as model molecule. Different types of experimental designs can be used, and in this work, a fractional factorial design (FFD) is proposed as it is a rapid and reliable tool, allowing the exploration of a maximum number of variables requiring less experimental observations than full factorial without a lack of main effects data [24]. Palmitoyl-L-carnitine, the selected model molecule, is an organic compound containing a long-chain acyl fatty acid with the carboxylic acid attached to carnitine through an ester bond. Its low solubility in water ($1.2e^{-05}$ g/L) makes it an excellent candidate to be used as a model hydrophobic therapeutic drug. As an active compound, palmitoyl-L-carnitine (pC) has been described for its capability of

altering the activity of various enzymes and transporters found in human membrane cells, and due to its role in fatty acid metabolism, it is also employed in research models to study mitochondrial function [25]. pC has also been reported to prevent biofilm formation in *Escherichia coli* and to target as well various pathways involved in *Pseudomonas aeruginosa* biofilm growth [26]. It has also been suggested that this molecule stimulates sphingosine-1-phosphate (S1P) receptors (S1PRs) which are becoming more widely recognized as important regulators of homeostasis and disease. S1PRs play a function in cell survival, migration, phenotypic, activation status, and proliferation in all biological systems [27].

2. MATERIALS

Polysorbate 80 (T80) (MW 428.6) and polysorbate 20 (T20) (MW 604.813) were kindly donated by Croda Iberica (Spain). Palmitoyl-L-carnitine (pC) (MW 399.61) (≥97% HPLC), (±)-α-Tocopherol (TOC) (MW 430.71) (≥96% HPLC) and Octadecylamine (ODA) (MW 269.51) as well P10 desalting columns (bed size 14.5 mm x 50 mm) were purchased from Sigma-Aldrich (Spain). DiD' oil (1,1'-Dioctadecyl-3,3,3',3'-Tetramethylindodicarbocyanine Perchlorate) was purchased from Fisher Scientific (Spain). Phosphate-buffered saline (PBS) and D-mannitol were purchased from Sigma-Aldrich (Spain). Acetic acid (Scharlab, Spain), potassium hydroxide (Sigma-Aldrich, Spain), potassium phosphate monobasic (Sigma-Aldrich, Spain) and sodium phosphate dibasic (Sigma-Aldrich, Spain) were used to prepare different buffers. Vivaflow 50 Cassettes (Regenerated Cellulose, 100 KDa) and 0,2 µm filters (Regenerated Cellulose) were purchased from Sartorius Stedim Biotech (Germany). Acetonitrile HPLC Supragradient was purchased from Scharlab (Spain). Other chemicals were of analytical reagent grade and used without further purification.

3. METHODS

3.1. Surfactant screening

The initial aim was to select the best surfactant for NE formation, thus two non-ionic surfactants, T80 and T20, were evaluated for their ability to form stable free-drug nanoemulsions (Blank NE). The method used for preparation of NE was the solvent injection technique reported earlier by Schubert *et al.* [28]. Briefly, 250 µl of ethanol solution containing TOC (5 mg) and ODA (1 mg) were prepared. Surfactants were also added into the ethanol solution at different amounts (0.1 mg, 0.5 mg, 5 mg, and 10 mg). The organic phase was then injected into 1 ml of phosphate-buffered saline (PBS 1x) solution at RT under continuous stirring (700 rpm) in order to form the NE. The resulting NE were purified by size exclusion chromatography, using P10 desalting columns.

3.2. Identification of critical variables by QbD approach

After selection of the best surfactant, a quality by design (QbD) approach using Design of Experiments (DoE) was implemented for screening and designing pC-loaded nanoemulsions (pC-NE) (Design Expert v. 12.1). A two-level fractional factorial design (resolution IV) was selected as model: four independent variables (final concentration of TOC, ODA, T80 and pC) and three dependent variables (hydrodynamic diameter, polydispersity index and zeta potential) were defined and levels for each factor were established (Table 1), with addition of 3 center points (level 0) used to test for curvature. The selected model required the preparation of nineteen pC-NE which were synthetized by the addition of pC to 250 µl of ethanol solution containing TOC, ODA, and T80. The procedure was the same as described for the synthesis of blank NE in 3.1. Later, the obtained data were analyzed using Pareto charts and half-normal plots, followed by ANOVA analysis, in order to identify the factors exhibiting the highest influence on the chosen critical quality attributes (CQAs). Finally, the analysis of obtained results using DoE allowed us to predict two optimal pC-NE compositions according to the desired

physico-chemical properties, that were further developed and studied (pC-NE_T and pC-NE_U formulations).

Table 1. Selected variables levels for palmitoyl-carnitine loaded nanoemulsions screening. The experimental levels (low and high) are represented by the coded values of -1 and +1, respectively, corresponding to the final concentration (mg/mL) of the components.

Independent variables	Variable codification	Level	
		-1	+1
TOC	A	2.5	7.5
ODA	B	0.15	0.85
pC	C	0.5	1.5
T80	D	0.25	1.75

3.3. Physicochemical characterization of NE

3.3.1. Particle size characterization

The hydrodynamic diameter and polydispersity index (PDI) of blank NE and pC-NE were assessed by photon correlation spectroscopy (PCS) using a Zetasizer nano ZS90 (Malvern Panalitical, UK). All measurements were performed in triplicates at RT.

3.3.2. Determination of zeta potential

The surface charge of pC-NE was determined by Electrophoretic Light Scattering (ELS) using a Zetasizer Nano ZS90 (Malvern Instruments, UK). The nanosuspensions synthesized in PBS were diluted (1:10) in ultrapure water prior to zeta potential analysis, whereas those synthesized in ultrapure water were diluted (1:20) in sodium chloride 100 mM prior to zeta potential analysis. Each sample was analyzed in triplicates at RT.

3.3.3. Morphology determination by transmission electron microscopy

The morphology of pC-NE (formulations pC-NE_T and pC-NE_U) was examined by transmission electron microscopy (TEM). TEM analyses were performed at the National Centre of Electronic Microscopy of the Complutense University of Madrid (UCM, Madrid, Spain). NE were placed on the surface of carbon-coated copper grids, negatively stained with 2% uranyl acetate and observed under TEM using a JEOL JEM 1400 instrument operated at 100 kV equipped with a CCD camera Gatan Orius Sc 200.

3.4. Stability studies

Both pC-NE_T and pC-NE_U formulations were subjected to stability studies in triplicate. The physical stability in PBS of both NE was evaluated following storage at 4ºC and RT, by measurement of hydrodynamic diameter, PDI and zeta potential at preestablished time-points during 2 weeks. Moreover, the behavior of pC-NE_U formulation was also investigated in ultrapure water at 4ºC and RT and at different pH conditions (pH 7.4 and pH 5.3) up to 4 months.

3.5. Determination of entrapment efficiency of pC-NE

The concentration of pC in pC-NE_U formulation was determined before and after purification process after synthesis through HPLC-RID analysis using a Waters Symmetry C18 column (4.6x75 3.5um). The chromatography was carried out in Agilent 1260 system, at a flow rate 1 mL/min in isocratic conditions, where the mobile phase was acetonitrile/ KH_2PO_4 (50 mM) (65:35 v/v) at pH = 3.5 adjusted with o-phosphoric acid. For NE disruption and sample preparation see supporting info. Entrapment efficiency (EE) was calculated using the following formula:

$$EE\ (\%) = \frac{C_{AP}}{C_{BP}}\ X\ 100$$

where C_{AP} is the pC concentration found in disrupted NE after the purification process and C_{BP} is the pC concentration found in disrupted NE before the purification process.

3.6. Determination of reaction yield and loading content of pC-NE

For determining the yield of the synthesis process resulting in NE formation, NE_U formulations (both blank and pC-NE_U) were synthetized as previously described and resulting purified formulations were lyophilized and accurately weighted to obtain the total mass of NE (m_{exp}). This experiment was done in triplicate. The reaction yield (R) was calculated as follows:

$$R\ (\%) = \frac{m_{exp}}{m_{the}}\ X\ 100$$

Where m_{exp} is the total mass of NE found after the purification process and m_{the} is the theoretical total mass of NE.

The loading capacity (LC) in pC-NE_U was calculated using the EE as follows:

$$LC\ (\%) = \frac{EE\ X\ total\ pC\ amount}{m_{exp}}\ X\ 100$$

3.7. pC-NE_U formulation biodistribution

For biodistribution studies, pC-NE_U was synthesized in mannitol (5.5% w/v) and loaded with DiD' oil, a near infrared fluorescent dye, adding it in the organic phase. The fluorescent formulation was characterized by measuring hydrodynamic size, polydispersity index and zeta potential, as previously described. The entrapment efficiency (EE) of the dye was determined spectrophotometrically using a Clariostar microplate reader using the same formula than for pC entrapment efficiency (see 3.5). Biodistribution studies were performed on healthy mice. For that purpose, four C57BL/6 mice were intravenously injected with the fluorescent pC-NE_U formulation (DiD-pC-NE_U). In addition, one C57BL/6 mouse was left non-injected as control. Four hours post injection, mice were sacrificed, perfused using 4% formaldehyde and dissected. Dissected tissues, including brain, heart, lungs, stomach, spleen, liver, bladder, kidneys, muscle and bone were then analyzed using an *ex vivo* fluorescence imaging system. Animal experiments were conducted according to Spanish and EU regulations (PROEX277/16).

4. RESULTS AND DISCUSSION

4.1. Effect of surfactants on nanoemulsions characteristics

The surfactant type plays a critical role in the formation of small and stable NE [29]. We studied the effect of two surfactants, T20 and T80, on particle size and distribution. Increase in T20 concentration from 0.1 to 10 mg/mL (F5-F8) caused a drastic particle size decrease from more than 700 nm to about 250 nm for NE, as shown in Table 2. The difference between these two values was due to the presence of aggregates in F5 as the lack of stabilizing surfactant triggered particles aggregation. On the other hand, when using T80 the situation was quite different, with smaller particle sizes in all concentrations tested compared to T20, as depicted in Table 2. Moreover, increasing T80 concentration from 1 mg to 10 mg/mL (F2-F4) resulted in slightly larger particles but significant increase of polydispersity, this could be explained by a reduced diffusion rate of the molecules in the sample caused by an increased viscosity of the continuous phase. The different behavior of both surfactants can be explained by the nature of intermolecular interaction stablished. Both polysorbates have a common backbone and only differ in the structures

of the fatty acid sidechains, oleic acid in the case of T80, lauric acid for T20. In fact, the fatty acid chain length and degree of unsaturation in the surfactant influence particle size [30]. The fatty acid with shorter chain length is more rigid and tends to form larger particles with lower curvature. Moreover, the higher the number of unsaturation in the hydrocarbon chain, the more flexible is the chain and smaller the particles obtained. Smaller particle size was obtained for NE containing T80 probably due to the bend and kink effect at the double bond of monooleate, which increased the curvature of NE droplets [31]. Thus, based on the size and polydispersity index obtained for all the synthesized batches, T80 was selected as the best surfactant for stabilizing the NE.

Table 2. Effect of surfactants polysorbate 80 (T80) and 20 (T20) concentration on the particle size and polydispersity of NE (mean ± SD, n=3).

Lipid	Sample code	T80 (mg/mL)	T20 (mg/mL)	Mean particle size (nm)	PDI
TOC ODA	F1	0.1	-	304 ± 4	0.274 ± 0.014
	F2	1	-	240 ± 4	0.200 ± 0.013
	F3	5	-	255 ± 4	0.280 ± 0.021
	F4	10	-	279 ± 3	0.504 ± 0.036
	F5	-	0.1	700 ± 5	0.302 ± 0.040
	F6	-	1	320 ± 3	0.200 ± 0.024
	F7	-	5	295 ± 4	0.230 ± 0.017
	F8	-	10	246 ± 4	0.370 ± 0.023

4.2. Analysis of critical variables by DoE

Design of experiments is a popular and widely used research approach for determining the critical factors affecting a process, e.g., the nanoparticles production. A fractional factorial design with resolution IV was selected as model $(2\,^{4-1}_{IV})$. The power of the model was 95.3% for all evaluated effects, ensuring its suitability, and it is adjusted to a general linear model and its double interactions. It required the synthesis and characterization of nineteen formulations (for composition see supporting info, Table S1), encoded A-S: most of the samples showed small hydrodynamic sizes (180-300 nm), narrow size distribution (PDI<0.3) and positive zeta potential (Figure 1).

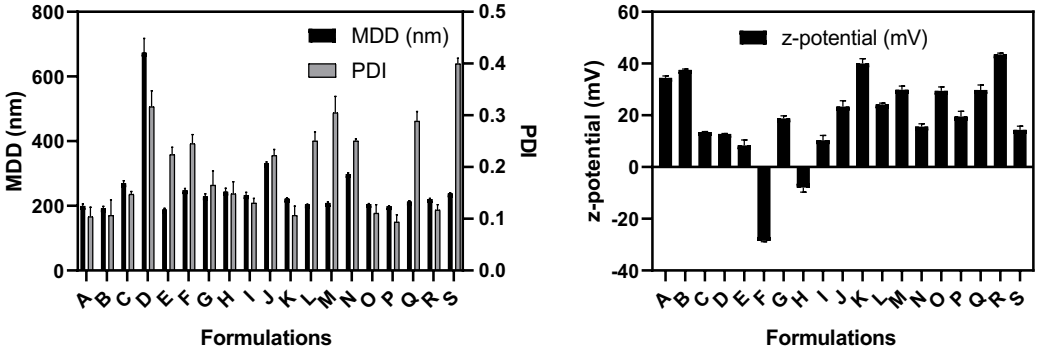

Figure 1. Particle size, polydispersity index and zeta potential of pC-NE formulations. MDD: Mean droplet diameter; PDI: polydispersity index, z-potential: Zeta potential

4.2.1. Effect of independent variables on size

Analysis of variance showed that the model was significant (F-value = 3.29) with a lack of fit not significant relative to the pure error. Among the evaluated independent variables, tocopherol content (variable A) was the only one statistically significant influencing particle size (p=0.02). An increase in the oil amount is associated with the increase of particle size, which can be compensated with the addition of higher amount

of the surfactant (T80) and/or the co-surfactant (ODA), as showed in the diagram for these interactions displayed in Figure 2 (I and II, red lines), so the interaction of variables AD (TOC-T80) and AB (TOC-ODA) influenced the size in somehow.

4.2.2. Effect of independent variables on polydispersity index (PDI)

As for the size, analysis of variance showed that the model was significant (F-value=9.54) with a lack of fit not significant relative to the pure error. Among the evaluated independent variables, the influence of individually evaluated variables on PDI have not statistical significance, whereas the interactions of variables AB and AD had big impact on PDI, with p-values much lower than 0.05 (AB p-value=0.008; AD p-value<0.0001). The use of an excess of surfactant or co-surfactant has a negative impact on population homogeneity with higher PDI values, which can be ameliorated increasing the oil content in the formulation, as showed in the diagram for these interactions displayed in Figure 3 (I and II, red lines).

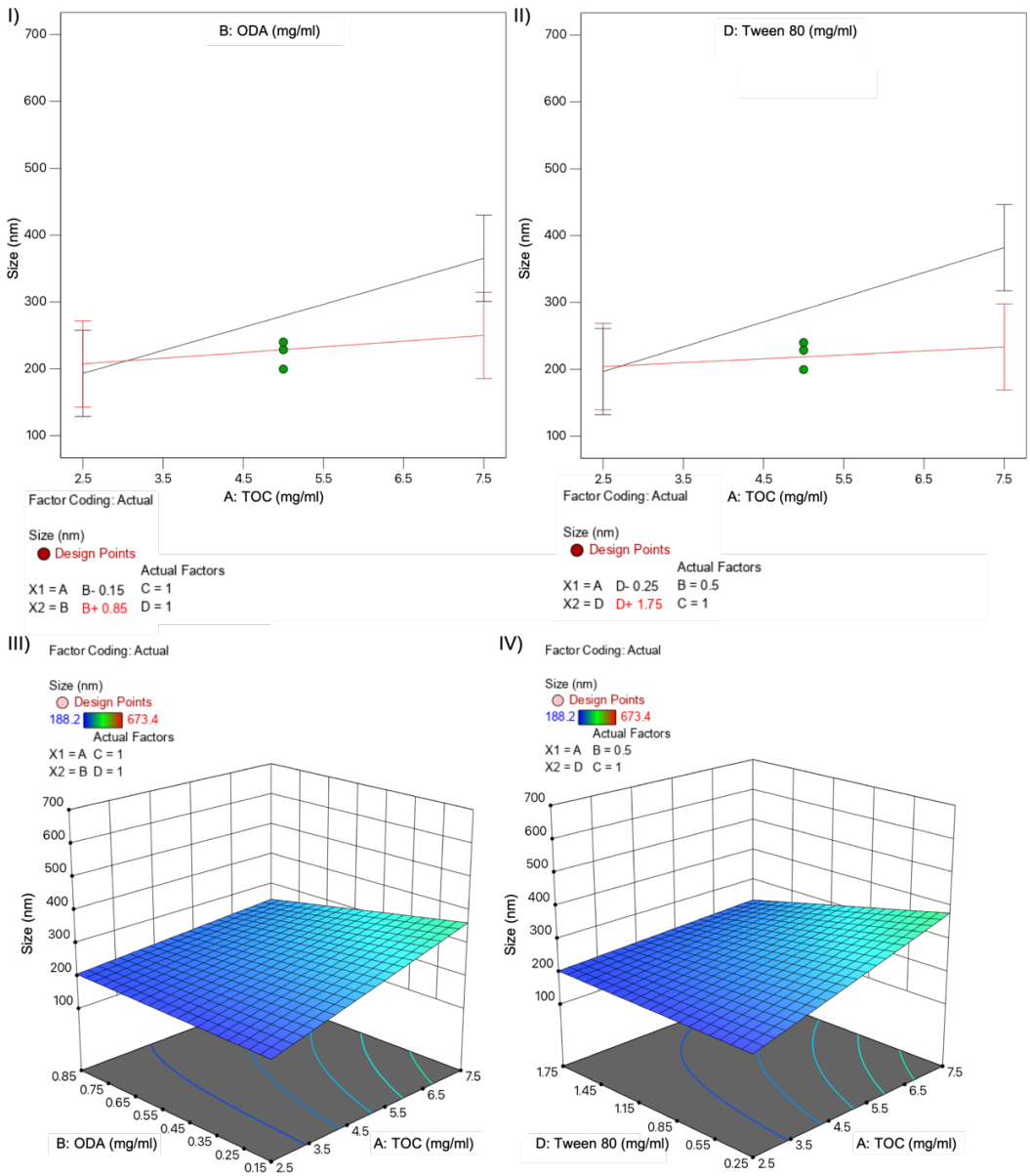

Figure 2. Normal plots (I-II) and 3D surface diagram (III-IV) for variable interactions influencing particle size: TOC-ODA (I and III) and TOC-T80 (II and IV).

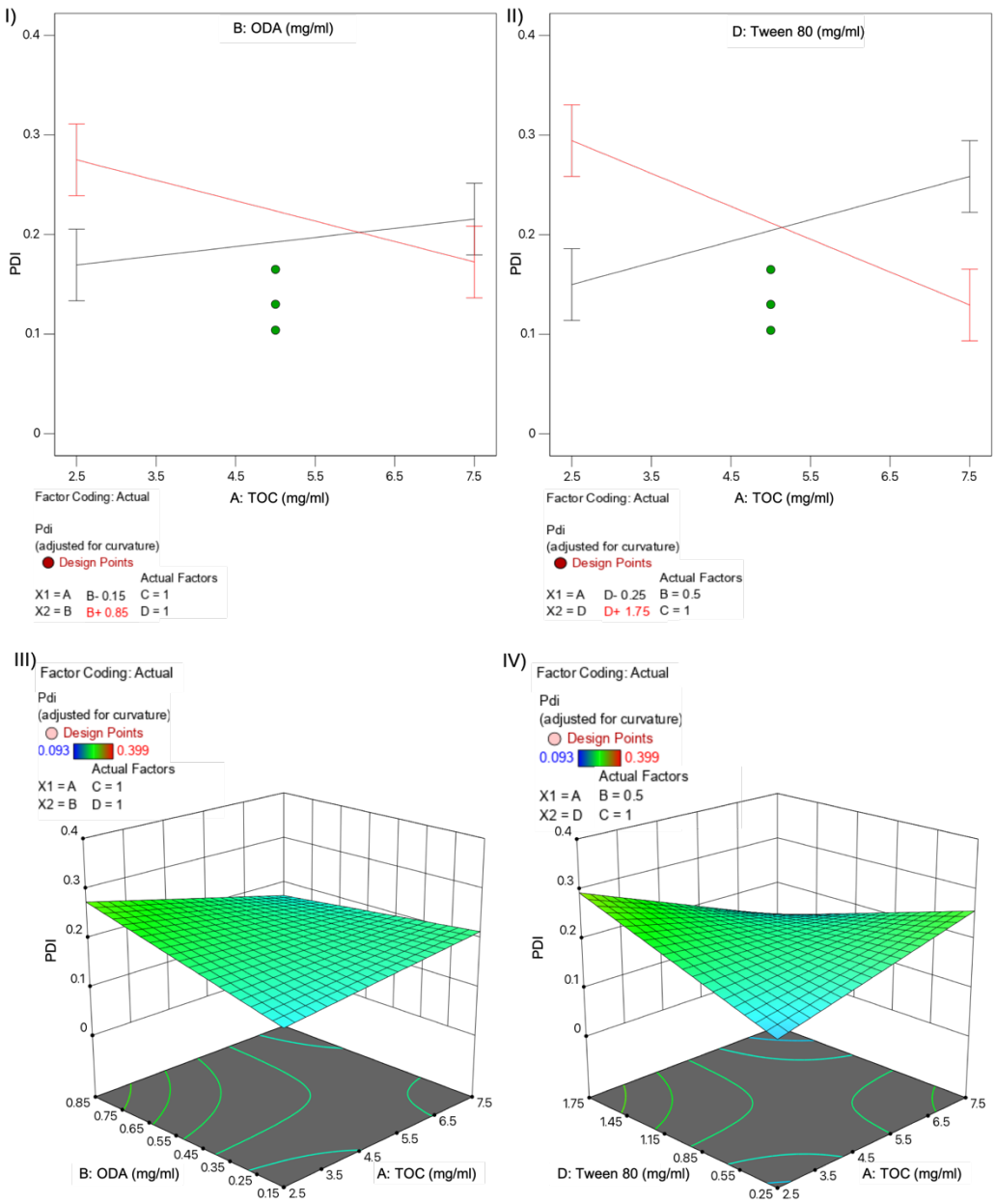

Figure 3. Normal plots (I-II) and 3D surface diagram (III-IV) for variable interactions influencing polydispersity index: TOC-ODA (I and III) and TOC-T80 (II and IV).

4.2.3. Effect of independent variables on zeta potential

For zeta potential evaluation, the model was also significant according to the analysis of variance (F-value=3.43), with a lack of fit not significant relative to the pure error. Among the evaluated independent variables, pC content (variable C) is the only one with statistically significant influence in the zeta potential (p-value=0.044), which is slightly influenced by the interactions involving TOC (AC and AD with p-value=0.069). Content in ODA has an impact on zeta potential due to its cationic nature, but it is not significant in the model (p-value=0.18). Figure 4 displays influence of single factors, whereas 3D surface diagram for interaction AC is displayed in Figure 5.

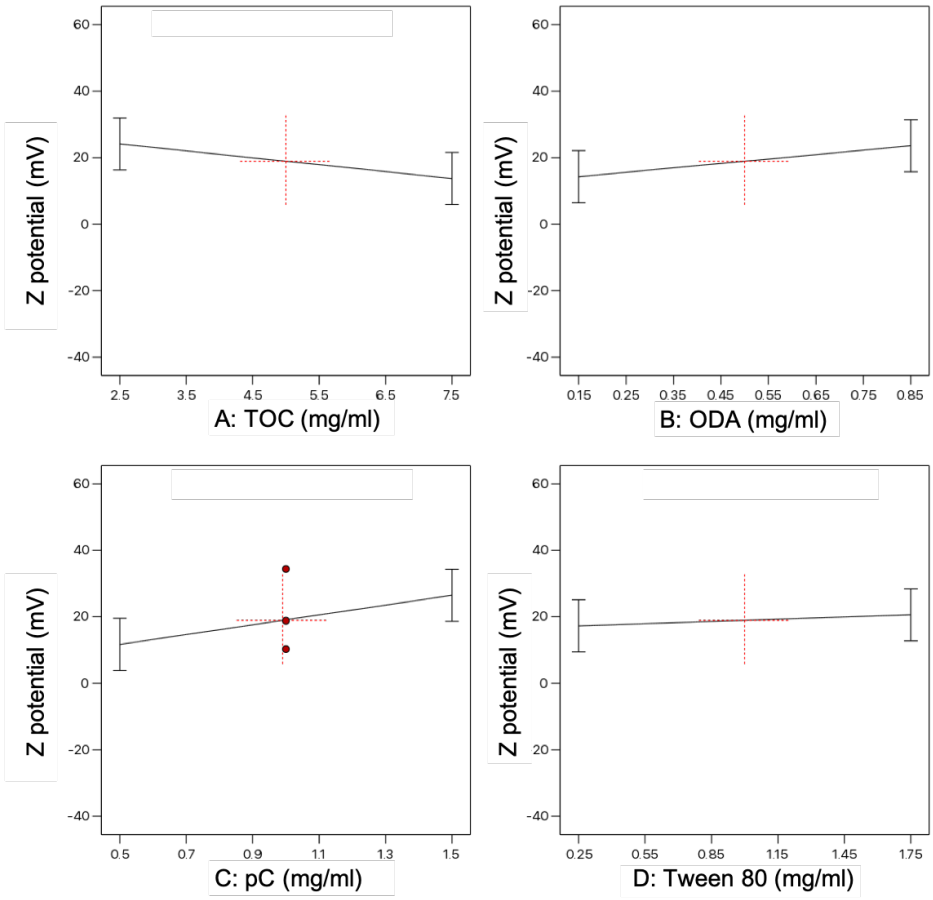

Figure 4. Main effect plot showing the effect of individual variables on zeta potential.

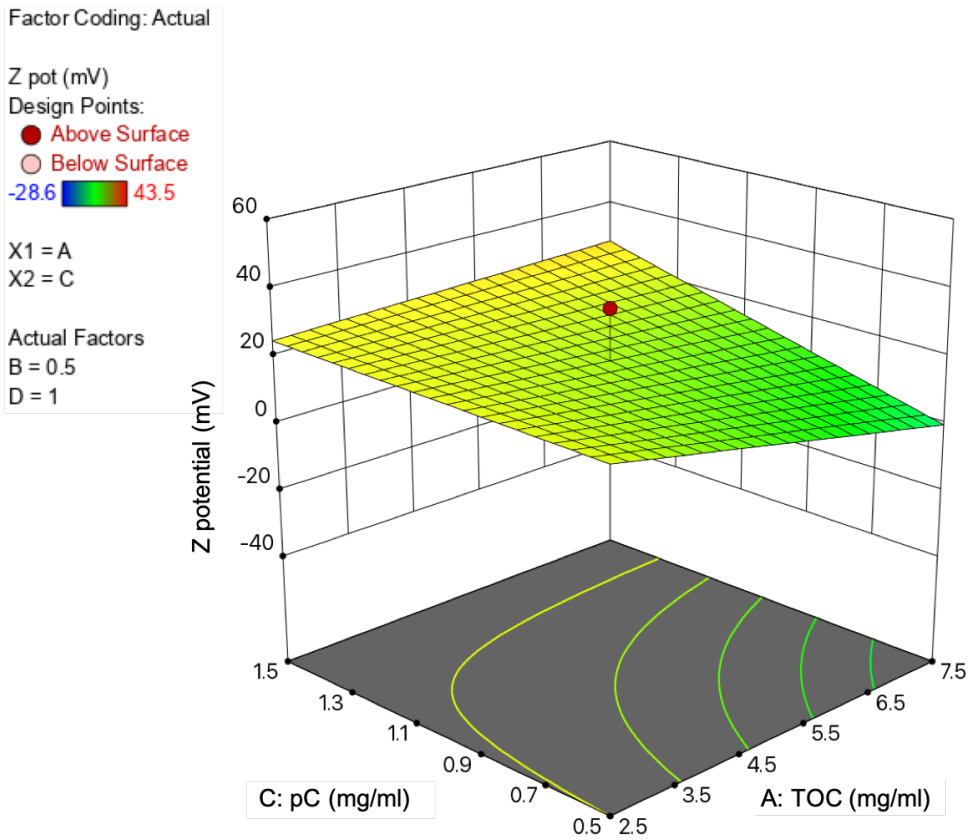

Figure 5. Zeta potential 3D surface diagram for variables A and C interaction.

4.2.4. Formulations optimization and prediction

After the analysis of data collected from the screening, an optimization was carried out introducing in the software several criteria concerning desired ranges for several parameters. The first optimization criteria were: size in range between 150 and 200 nm, PDI in range between 0.09 and 0.2, and zeta potential in range between +30 and +45 mV, as positive surface charge may be desirable to increase the interaction of the nanocarrier with cellular membranes [32–34]. In a second optimization run we maintained these criteria but included a further constrain to maximized TOC content, as increasing the lipid phase should increase the chances for hydrophobic model molecule incorporation. In the first optimization we obtained 84 solutions, 12 of them with desirability 1, whereas in the second optimization run we obtained 74 solutions, but the highest desirability was 0.62, indicating that the prediction may be not so accurate. A confirmation test was performed by synthesis of 2 of the optimized compositions in triplicate, encoded as formulation pC-NE_T (prediction 1) and formulation pC-NE_U (prediction 2) respectively. As shown in table 3, observed responses for both pC-NE_T and pC-NE_U formulations agreed with predicted values and were within the confidence intervals bounds, showing the suitability of selected DoE model. Formulations with these compositions were used for further characterization.

Table 3. Composition of optimized formulations pC-NE_T and pC-NE_U: predicted and experimental values (observed mean) for hydrodynamic size (MDD), PDI and zeta potential (ZP).

Code	Composition	Amount (mg)	Responses	Predicted mean	95% CI low for mean	95% CI high for mean	Observed mean (mean ± SD, n=3)
pC-NE_T	TOC	2.5	MDD (nm)	199.0	106.9	291.1	184.6 ± 7.5
	ODA	0.62	PDI	0.168	0.117	0.219	0.095 ± 0.006
	T80	0.25	ZP (mV)	+31.8	+15.9	+47.8	+21.7 ± 2.0
	pC	0.5					
pC-NE_U	TOC	7.5	MDD (nm)	175.6	65.4	285.9	255.9 ± 7.8
	ODA	0.85	PDI	0.108	0.047	0.170	0.131± 0.010
	T80	1.75	ZP (mV)	+29.7	+12.3	+47.1	+37.8 ± 1.2
	pC	1.1					

CI: Confidence interval bounds

4.3. Physico-chemical characterization of pC-NE

Three independent batches of pC-NE_T and pC-NE_U were synthetized as previously described in the experimental section (see Table 2 for summary of physico-chemical characterization by PCS). Both compositions (pC-NE_T and pC-NE_U) were smaller than 300 nm with very low polydispersity index (PDI<0.15) which indicates the homogeneity of size distribution. The zeta potential of pC-NE_T and pC-NE_U was also determined, being around +22 mV for formulation pC-NE_T and higher in the case of formulation pC-NE_U, close to +40 mV. This result is likely due to differences in composition among both formulations, as formulation pC-NE_U contains higher concentration of cationic compounds (ODA and pC) influencing zeta potential [35].

The morphological analysis of formulations pC-NE_T and pC-NE_U was performed by TEM. Both NE showed a spherical shape with a narrow size distribution (Figure 6) which is consistent with the size determined by PCS (Table). Furthermore, no large aggregates were observed, indicating homogeneous particle populations, corresponding with low polydispersity indexes obtained by PCS.

Due to its stability behavior (see 4.4), we only determined the effective chemical composition of formulation pC-NE_U, through determination of synthesis process yield, entrapment efficiency and loading capacity. The yield of the synthesis reaction for NE_U formulations (blank and pC-loaded) was 83.3 ± 4.9 % and 81 ± 5 % (n=3) respectively, demonstrating the suitability of the solvent injection technique as synthesis method for the development of these NE. The entrapment efficiency and loading capacity of pC in pC-NE_U was high as well, obtaining 89.7 ± 6.3 % and 14 ± 0.36 % (n=3) respectively, confirming the ability of the designed NE to incorporate the hydrophobic model compound in an efficient manner.

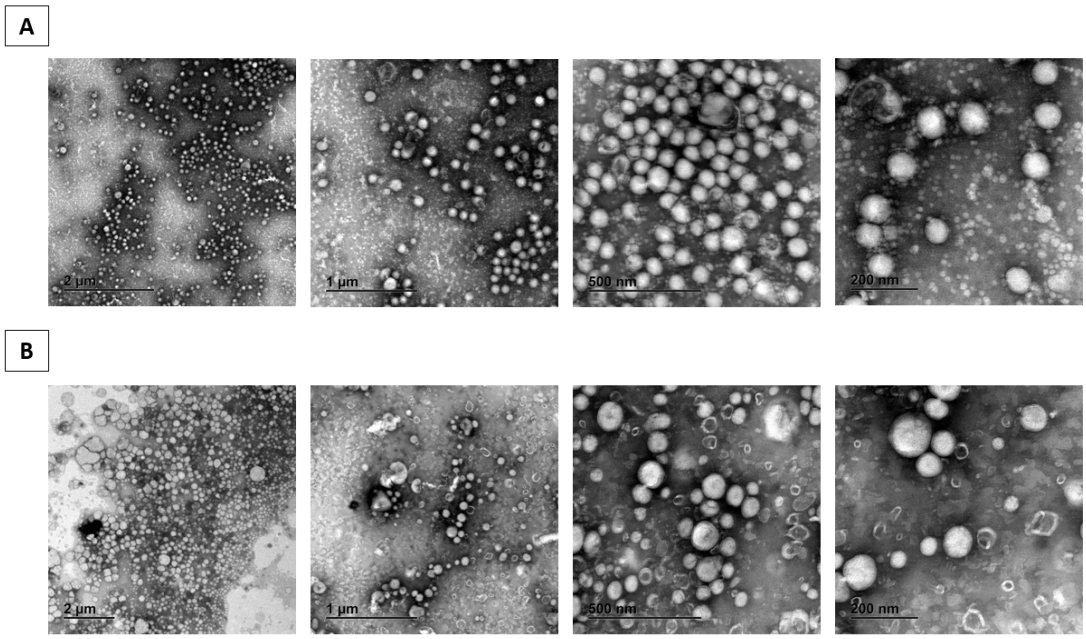

Figure 6. TEM images of pC-NE_T (A) and pC-NE_U (B) formulations.

4.4. Stability studies

The physical stability of both pC-NE_T and pC-NE_U formulations was evaluated in PBS following storage at 4ºC and RT for 2 weeks. PBS was selected as a relevant buffer for future biological studies. No significant change in the particle size and PDI of NE was observed except for formulation pC-NE_T stored at RT, which increased both parameters over time, with a size close to 500 nm after two weeks (Figure 7) indicating that particle's aggregation is influenced by temperature.

All of the NE, except for pC-NE_U stored at 4ºC, showed a decrease in zeta potential, reaching negative values after five days, which indicates that refrigerated storage is more appropriate to keep cationic surface charge for longer time. Differences found in stability behavior between both compositions may be related to the different zeta potential showed by formulation pC-NE_T and pC-NE_U. The surface charge of particles plays an important role in their physical stability as it may influence the rate of aggregation and fusion among particles. It has been suggested that full electrostatic stabilization requires a zeta potential higher than 30 mV in absolute values, being particles with potentials within that range more unstable and with higher tendency to flocculate. Although it is not

the unique parameter influencing colloidal stability of nanosuspensions [35], in the case of pC-NE_T (+22 mV) seems to have big impact in the showed short-term stability in PBS. According to stability results obtained for all the batches at the assessed conditions, pC-NE_U formulation was selected as the best pC-NE for the following experiments.

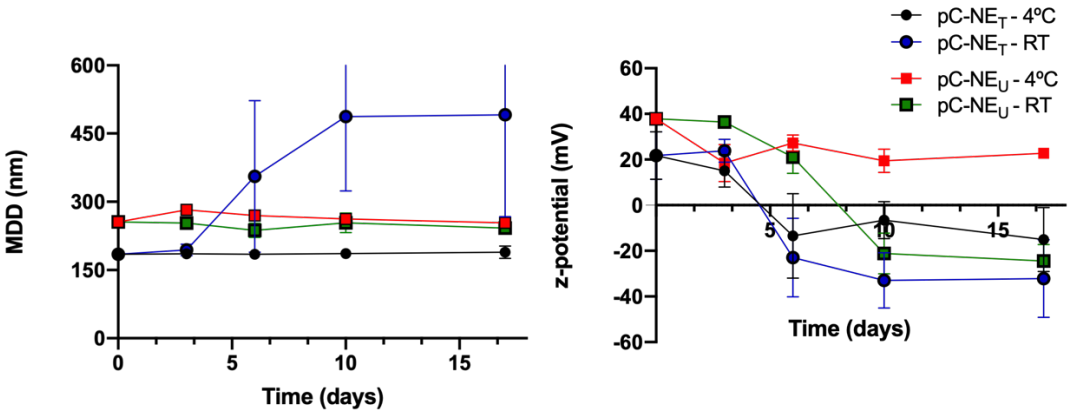

Figure 7. Effect of storage conditions on particle size and zeta potential on pC-NE_T and pC-NE_U formulations in PBS 1x (mean±SD, n=3).

To study the long-term stability of this composition, NE_U formulations (both blank and pC-loaded) were synthesized and stored in ultrapure water at 4ºC and RT for four months, being evaluated at pre-stablished time points (Figure 8). Particle size was significantly smaller (174 ± 30 nm) when NE was prepared in ultrapure water instead of PBS. The different size between NE obtained in ultrapure water and PBS could be explain by the nature of intermolecular interaction stablished. According to DLVO theory, in ultrapure water the electrostatic repulsion of NE is higher than van der Waals forces, thus they can remain dispersed during long time. However, due to the high ionic strength of PBS, the EDL is compressed and the electrostatic repulsion decreases inducing the size increase of the colloidal system [36]. No significant changes in particle size were observed for both NE when stored at 4ºC and RT, which is not surprisingly due to the low ionic strength of water compared to PBS. Zeta potential maintained positive during the whole period of study, although a reduction in the absolute value was observed in the formulations stored at RT.

pC-NE_U formulation stability was also evaluated under storage in low ionic strength buffers at pH 7.4 and pH 5.3. Figure 9 shows the evolution of hydrodynamic diameter and PDI over four months at those pH values. NE stored at pH 7.4 presented a decrease in zeta potential over time, reaching negative values after three weeks, which indicates that modifications in surface charge depend also on pH of surrounding environment. However, no significant changes were observed in particle size and zeta potential at pH 5.3, where NE presented also low PDI over time, thus indicating pC-NE_U nanoemulsions are potential candidates to be used as drug delivery systems for targeting disease environments in which acidic pH can be found, such tumors or infections sites. In fact, pH value is one of the critical variables involved in tumors, inflammations or infections in chronic wounds; it affects matrix metalloproteinase activity, fibroblast activity, keratinocyte proliferation, microbial proliferation, biofilm formation, and immunological responses [37–39].

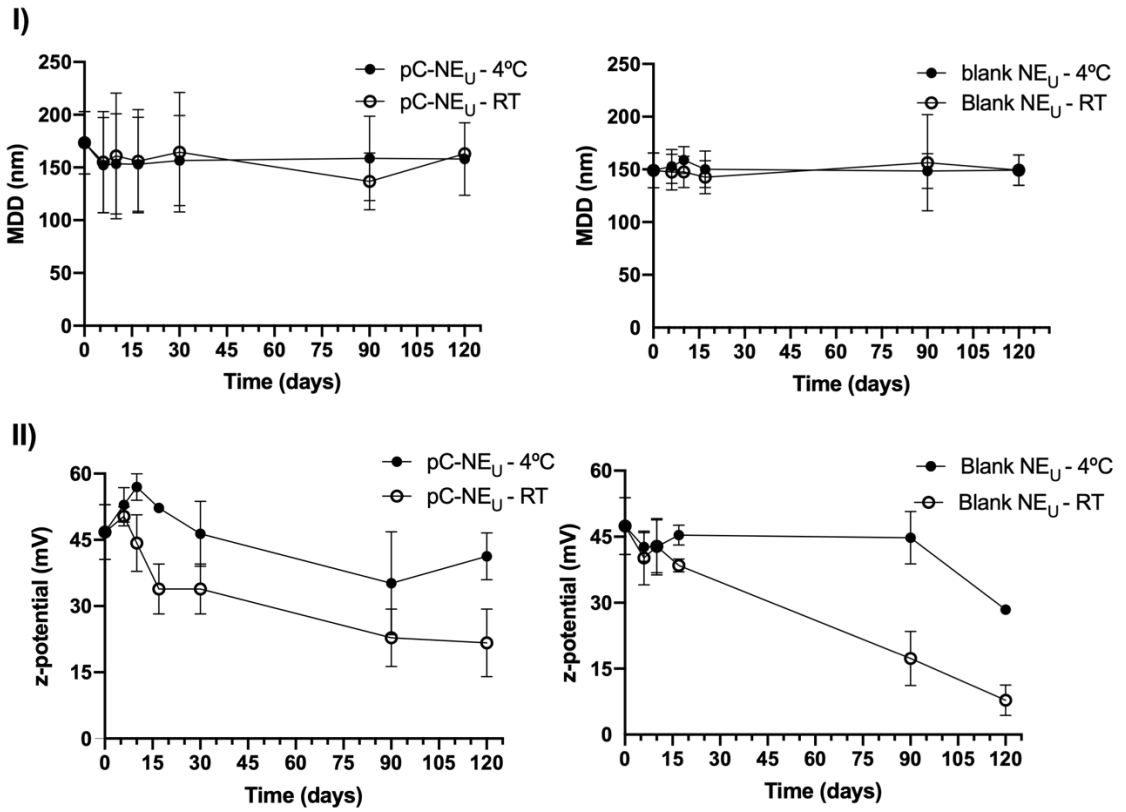

Figure 8. Effect of storage conditions on particle size (I) and zeta potential (II) on pC-NE_U and blank NE_U formulations in ultrapure water (mean±S.D., n=3).

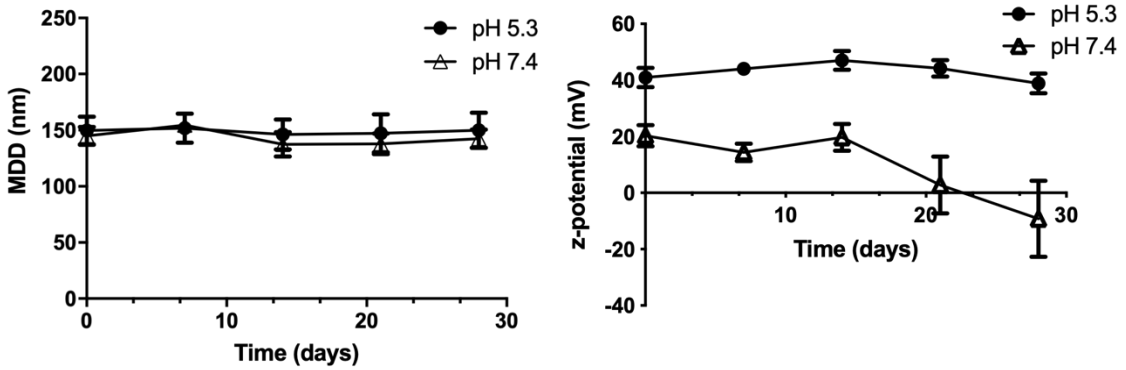

Figure 9. Effect of pH on particle size and zeta potential on pC-NE_U formulation (mean±S.D., n=3).

4.5. Scalability of the process

The reaction leading to the formation of Blank NE_U was subjected to a scale up process, increasing the compounds amount used in the small-scale synthesis up to 10 times. One of the keys to effective clinical use of nanoparticles is scaling up the nanoformulation process to manufacture large batches of samples. However, sometimes the desired features of nanoparticles are lost during the scale up of the reaction [40]. Nanoparticle formulations can increase the surface area by many folds and this may lead to very high aggregation after long periods of storage. The ratio between organic and aqueous phase

was kept constant. The synthesis procedure was the same to the one described for the synthesis of blank NE, except for stirring speed that was risen up to 1250 rpm. The resulting NE was purified by flow tangential filtration using Vivaflow Cassettes connected to a peristaltic pump (Watson-Marlow 323). We did not observe major change in initial physico-chemical properties (see supporting info, Table S2), which confirms a preserved functionality of Blank NE_U upon scaled up production. Figure 10 shows the physicochemical characteristics of scaled blank NE_U stored at both 4ºC and RT during 4 months. The stability behavior was comparable to the non-scaled up batches in terms of size, whereas the reduction of zeta potential in the formulations stored at RT was more marked in the scaled up samples.

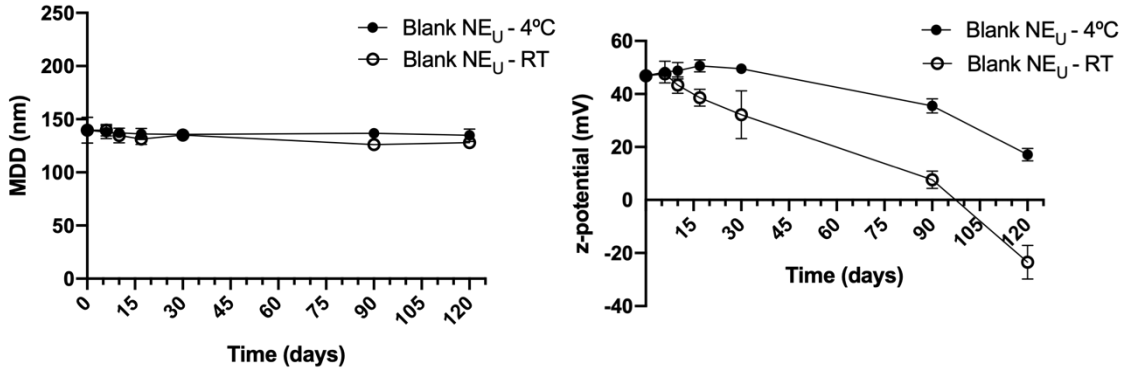

Figure 10. Effect of storage conditions on particle size and zeta potential on Blank NE_U formulations scaled up and stored in ultrapure water (mean±S.D., n=3).

4.6. *In vivo* distribution

A fluorescently labelled pC-NE_U was developed by adding DID' oil dye in the organic phase for studying its biodistribution in mice. The physicochemical properties of the fluorescent pC-NE_U formulation (DID-pC-NE_U) were not significantly different to those of non-fluorescent pC-NE_U formulation (see supporting info, Table S3). The entrapment efficiency of the dye was very high, close to 100%, confirming the affinity of this kind of dyes for the lipid core of the NE. Moreover, the stability of fluorescent labelling was studied up to 24h by incubation of DID-pC-NE_U in PBS at 37ºC. No release of fluorescent probe was detected (see supporting info, Figure S1), ensuring that observed signal in organs will be due to NE accumulation.

Four C57BL/6 mice were IV injected with DID-pC-NE_U; four hours post-injection, mice were sacrificed and after perfusion with 4% formaldehyde the fluorescence from dissected tissues was qualitatively measured (Figure). For this purpose, the dissected organs from a non-injected C57BL/6 mouse were used as control to eliminate the autofluorescence given by all tissues, thus leaving only the fluorescence produced by the injected NE. Live images of whole animals were not taken as they suffer from low light penetration into biological tissues. We found that DID-pC-NE_U formulation was predominantly accumulated in the liver, with minimal accumulation in spleen, stomach and kidneys. The combined activity of circulating blood moving through organs, as well as particle uptake by cells of the reticuloendothelial system (RES) recruited by these organs, could explain the high fluorescence recorded from the liver [41]. The liver is recognized to play an important part in the elimination and detoxification of different metabolites from the bloodstream, as well as lipid processing [42]. Similar biodistribution pattern have been described for NE ranging from 70-200 nm, as size has a crucial role in the *in vivo* fate of NE [43]. Moreover, Busman *et al.* have described that particle size influence accumulation in stomach after iv administration, finding the maximum accumulation in this organ for 150 nm NE compared to smaller NE [44], which is in agreement with our findings.

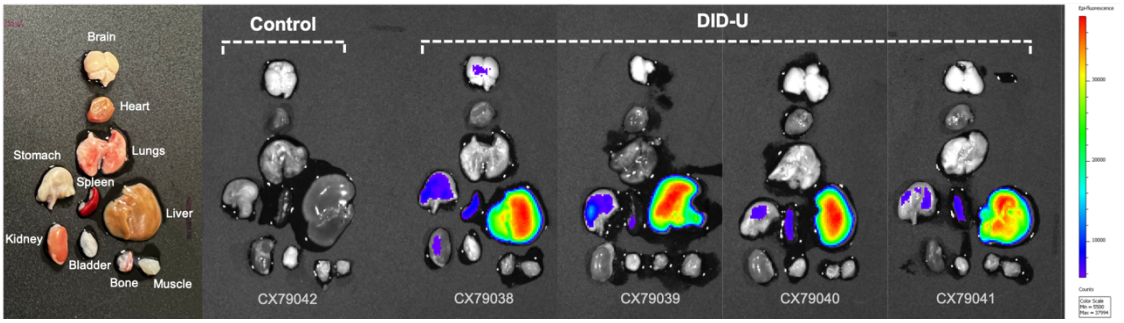

Figure 11. Ex vivo fluorescence imaging of dissected tissues from C57BL/6 mice non-injected (control) and four hours post injection with DiD conjugated pC-NE U. Fluorescence was adjusted using the non-injected mice as control in order to eliminate the natural autofluorescence given by all tissues.

5. CONCLUSIONS

Cationic nanoemulsions were successfully developed for the encapsulation of the hydrophobic model drug L-palmitoyl carnitine. The use of design of experiments approach appears as a useful tool for obtaining nanoemulsions with desired physico-chemical properties with minimized experimental effort, as previously reported [21–23]. One of the optimized compositions, pC-NE$_U$, led to a nanoemulsion with small hydrodynamic size (<200 nm), narrow size distribution (PDI<0.150) and high positive zeta potential (+40mV) which showed good stability profiles at different conditions of pH and temperature, and also after scaling up the synthesis process, which is highly desirable from a pharmaceutical industry point of view, ensuring an easier translation process [45]. Moreover, pC-NE$_U$ showed high entrapment capacity of L-palmitoyl carnitine, corroborating our initial hypothesis of the potential of nanoemulsions, if properly designed, as a drug delivery system for hydrophobic active compounds [46–48]. The biodistribution profile obtained is in line with those found by other authors for nanoemulsion with similar size [43,44], but it could be modulated changing physicochemical properties of the nanocarriers, such as size and surface composition [49].

In conclusion, the use of DoE allows for a rational design of drug delivery platforms. The simple composition of pC-NE$_U$, its easily prepared and the properties here showed make it a promising template for delivery of hydrophobic compounds, which may require an easy reformulation process depending on the drug.

Acknowledgements

We thank Laura Barrios from Secretaría General Adjunta de Informática (SGAI, CSIC) (Spain) for her help and suggestions for interpretation and discussion of design of experiments results, and Paolo Gasco from Nanovector Srl. (Italy) for his advices during chemical characterization of pC-NE$_U$, performed in Nanovector headquarters.

Funding

This work was supported by Atracción de Talento (Modalidad 1) program from Comunidad de Madrid (Spain) (Reference 2019-T1/IND-12906).

Author contributions

Conceptualization: AGP and FH; Methodology: All; Investigation: EAU, MMH and MLB; Data curation: EAU and AGP; Writing - original draft: EAU and AGP; Writing - review & Editing: All.

Bibliography

[1] Patra JK, Das G, Fraceto LF, Campos EVR, Rodriguez-Torres M del P, Acosta-Torres LS, et al. Nano based drug delivery systems: recent developments and future prospects. Journal of Nanobiotechnology. 2018 Dec;16(1):71.

[2] Thi TTH, Suys EJA, Lee JS, Nguyen DH, Park KD, Truong NP. Lipid-Based Nanoparticles in the Clinic and Clinical Trials: From Cancer Nanomedicine to COVID-19 Vaccines. Vaccines (Basel) [Internet]. 2021 Apr 8;9(4):359. Available from: https://pubmed.ncbi.nlm.nih.gov/33918072

[3] Mitchell MJ, Billingsley MM, Haley RM, Wechsler ME, Peppas NA, Langer R. Engineering precision nanoparticles for drug delivery. Nature Reviews Drug Discovery. 2021 Feb;20(2):101–24.

[4] Zielińska A, Carreiró F, Oliveira AM, Neves A, Pires B, Venkatesh DN, et al. Polymeric Nanoparticles: Production, Characterization, Toxicology and Ecotoxicology. Molecules. 2020 Aug;25(16):3731.

[5] Samimi S, Maghsoudnia N, Eftekhari RB, Dorkoosh F. Lipid-Based Nanoparticles for Drug Delivery Systems. In: Characterization and Biology of Nanomaterials for Drug Delivery [Internet]. Elsevier; 2019. p. 47–76. Available from: https://linkinghub.elsevier.com/retrieve/pii/B9780128140314000039

[6] Lu H, Zhang S, Wang J, Chen Q. A Review on Polymer and Lipid-Based Nanocarriers and Its Application to Nano-Pharmaceutical and Food-Based Systems. Frontiers in Nutrition. 2021 Dec;8.

[7] Dhiman N, Awasthi R, Sharma B, Kharkwal H, Kulkarni GT. Lipid Nanoparticles as Carriers for Bioactive Delivery. Frontiers in Chemistry. 2021 Apr;9.

[8] Shah R, Eldridge D, Palombo E, Harding I. Lipid Nanoparticles: Production, Characterization and Stability [Internet]. Cham: Springer International Publishing; 2015. (SpringerBriefs in Pharmaceutical Science & Drug Development). Available from: http://link.springer.com/10.1007/978-3-319-10711-0

[9] Kumar M, Bishnoi RS, Shukla AK, Jain CP. Techniques for Formulation of Nanoemulsion Drug Delivery System: A Review. Preventive Nutrition and Food Science. 2019 Sep;24(3):225–34.

[10] Wilson RJ, Li Y, Yang G, Zhao C-X. Nanoemulsions for drug delivery. Particuology [Internet]. 2022;64:85–97. Available from: https://www.sciencedirect.com/science/article/pii/S1674200121001176

[11] Guzmán E, Fernández-Peña L, Rossi L, Bouvier M, Ortega F, Rubio RG. Nanoemulsions for the Encapsulation of Hydrophobic Actives. Cosmetics. 2021 Jun;8(2):45.

[12] Sánchez-López E, Guerra M, Dias-Ferreira J, Lopez-Machado A, Ettcheto M, Cano A, et al. Current Applications of Nanoemulsions in Cancer Therapeutics. Nanomaterials. 2019 May;9(6):821.

[13] Yang G, Liu Y, Wang H, Wilson R, Hui Y, Yu L, et al. Bioinspired Core–Shell Nanoparticles for Hydrophobic Drug Delivery. Angewandte Chemie. 2019 Oct;131(40):14495–502.

[14] Louage B, Tack L, Wang Y, de Geest BG. Poly(glycerol sebacate) nanoparticles for encapsulation of hydrophobic anti-cancer drugs. Polymer Chemistry. 2017;8(34):5033–8.

[15] Klein S, Luchs T, Leng A, Distel L, Neuhuber W, Hirsch A. Encapsulation of Hydrophobic Drugs in Shell-by-Shell Coated Nanoparticles for Radio—and Chemotherapy—An In Vitro Study. Bioengineering. 2020 Oct;7(4):126.

[16] Liu Y, Yang G, Jin S, Xu L, Zhao C. Development of High-Drug-Loading Nanoparticles. Chempluschem. 2020 Sep;85(9):2143–57.

[17] Shakhwar S, Darwish R, Kamal MM, Nazzal S, Pallerla S, Abu Fayyad A. Development and evaluation of paclitaxel nanoemulsion for cancer therapy. Pharmaceutical Development and Technology. 2020 Apr;25(4):510–6.

[18] Prasad C, Bhatia E, Banerjee R. Curcumin Encapsulated Lecithin Nanoemulsions: An Oral Platform for Ultrasound Mediated Spatiotemporal Delivery of Curcumin to the Tumor. Scientific Reports. 2020 Dec;10(1):8587.
[19] Tinoco LM da S, da Silva FLO, Ferreira LAM, Leite EA, Carneiro G. Hyaluronic acid-coated nanoemulsions loaded with a hydrophobic ion pair of all-trans retinoic acid for improving the anticancer activity. Brazilian Journal of Pharmaceutical Sciences. 2018;54(4).
[20] Jain S. Quality by design (QBD): A comprehensive understanding of implementation and challenges in pharmaceuticals development. International Journal of Pharmacy and Pharmaceutical Sciences. 2014;6(1):29–35.
[21] González-Fernández FM, Bianchera A, Gasco P, Nicoli S, Pescina S. Lipid-based nanocarriers for ophthalmic administration: Towards experimental design implementation. Pharmaceutics [Internet]. 2021;13(4). Available from: https://www.scopus.com/inward/record.uri?eid=2-s2.0-85103880697&doi=10.3390%2Fpharmaceutics13040447&partnerID=40&md5=c6b0ba129366f9f06efa6afb24260cda
[22] Lee R. Statistical Design of Experiments for Screening and Optimization. Chemie Ingenieur Technik [Internet]. 2019 Mar 1;91(3):191–200. Available from: https://doi.org/10.1002/cite.201800100
[23] Tavares Luiz M, Santos Rosa Viegas J, Palma Abriata J, Viegas F, Testa Moura de Carvalho Vicentini F, Lopes Badra Bentley MV, et al. Design of experiments (DoE) to develop and to optimize nanoparticles as drug delivery systems. European Journal of Pharmaceutics and Biopharmaceutics. 2021;165:127–48.
[24] Kuncahyo I, Choiri S, Fudholi A, Martien R, Rohman A. Assessment of Fractional Factorial Design for the Selection andScreening of Appropriate Components of a Self-nanoemulsifyingDrug Delivery System Formulation. Advanced Pharmaceutical Bulletin [Internet]. 2019;9(4):609–18. Available from: https://apb.tbzmed.ac.ir/Article/apb-27674
[25] Bernatoniene J, Majiene D, Peciura R, Laukeviciene A, Bernatoniene R, Mekas T, et al. The effect of Ginkgo biloba extract on mitochondrial oxidative phosphorylation in the normal and ischemic rat heart. Phytother Res [Internet]. 2011 Jul;25(7):1054–60. Available from: http://www.ncbi.nlm.nih.gov/pubmed/21259351
[26] Wenderska IB, Chong M, McNulty J, Wright GD, Burrows LL. Palmitoyl-dl-Carnitine is a Multitarget Inhibitor of Pseudomonas aeruginosa Biofilm Development. ChemBioChem [Internet]. 2011 Dec;12(18):2759–66. Available from: http://doi.wiley.com/10.1002/cbic.201100500
[27] Blaho VA, Hla T. An update on the biology of sphingosine 1-phosphate receptors. Journal of Lipid Research [Internet]. 2014 Aug 1;55(8):1596–608. Available from: https://doi.org/10.1194/jlr.R046300
[28] Schubert MA, Müller-Goymann CC. Solvent injection as a new approach for manufacturing lipid nanoparticles – evaluation of the method and process parameters. European Journal of Pharmaceutics and Biopharmaceutics. 2003;55(1):125–31.
[29] Gupta A, Eral HB, Hatton TA, Doyle PS. Nanoemulsions: formation, properties and applications. Soft Matter [Internet]. 2016;12(11):2826–41. Available from: http://xlink.rsc.org/?DOI=C5SM02958A
[30] Eh Suk VR, Mohd. Latif F, Teo YY, Misran M. Development of nanostructured lipid carrier (NLC) assisted with polysorbate nonionic surfactants as a carrier for l-ascorbic acid and Gold Tri.E 30. Journal of Food Science and Technology [Internet]. 2020 Mar; Available from: http://link.springer.com/10.1007/s13197-020-04357-x
[31] Saberi AH, Fang Y, McClements DJ. Fabrication of vitamin E-enriched nanoemulsions: Factors affecting particle size using spontaneous emulsification.

Journal of Colloid and Interface Science [Internet]. 2013;391:95–102. Available from: https://www.sciencedirect.com/science/article/pii/S0021979712011228
[32] González-Paredes A, Sitia L, Ruyra A, Morris CJ, Wheeler GN, McArthur M, et al. Solid lipid nanoparticles for the delivery of anti-microbial oligonucleotides. European Journal of Pharmaceutics and Biopharmaceutics [Internet]. 2019;134:166–77. Available from: https://www.sciencedirect.com/science/article/pii/S0939641118308385
[33] Nazarenus M, Zhang Q, Soliman MG, del Pino P, Pelaz B, Carregal-Romero S, et al. In vitro interaction of colloidal nanoparticles with mammalian cells: What have we learned thus far? [Internet]. Vol. 5, Beilstein journal of nanotechnology. Fachbereich Physik, Philipps-Universität Marburg, Renthof 7, 35037 Marburg, Germany.; 2014. p. 1477–90. Available from: http://europepmc.org/abstract/MED/25247131
[34] Åberg C, Piattelli V, Montizaan D, Salvati A. Sources of variability in nanoparticle uptake by cells. Nanoscale [Internet]. 2021;13(41):17530–46. Available from: http://dx.doi.org/10.1039/D1NR04690J
[35] Wang P, Keller AA. Natural and Engineered Nano and Colloidal Transport: Role of Zeta Potential in Prediction of Particle Deposition. Langmuir. 2009 Jun;25(12):6856–62.
[36] Moore TL, Rodriguez-Lorenzo L, Hirsch V, Balog S, Urban D, Jud C, et al. Nanoparticle colloidal stability in cell culture media and impact on cellular interactions. Chemical Society Reviews [Internet]. 2015;44(17):6287–305. Available from: http://xlink.rsc.org/?DOI=C4CS00487F
[37] Fulaz S, Vitale S, Quinn L, Casey E. Nanoparticle–Biofilm Interactions: The Role of the EPS Matrix. Trends in Microbiology [Internet]. 2019 Nov;27(11):915–26. Available from: https://linkinghub.elsevier.com/retrieve/pii/S0966842X19301854
[38] Percival SL, McCarty S, Hunt JA, Woods EJ. The effects of pH on wound healing, biofilms, and antimicrobial efficacy. Wound Repair and Regeneration. 2014 Mar;22(2):174–86.
[39] Mu H, Tang J, Liu Q, Sun C, Wang T, Duan J. Potent Antibacterial Nanoparticles against Biofilm and Intracellular Bacteria. Scientific Reports [Internet]. 2016 May;6(1):18877. Available from: http://www.nature.com/articles/srep18877
[40] Paliwal R, Babu RJ, Palakurthi S. Nanomedicine scale-up technologies: feasibilities and challenges. AAPS PharmSciTech. 2014 Dec;15(6):1527–34.
[41] Kumar R, Roy I, Ohulchanskky TY, Vathy LA, Bergey EJ, Sajjad M, et al. iIn Vivo/i Biodistribution and Clearance Studies Using Multimodal Organically Modified Silica Nanoparticles. ACS Nano. 2010 Feb;4(2):699–708.
[42] Mannucci S, Boschi F, Cisterna B, Esposito E, Cortesi R, Nastruzzi C, et al. pA Correlative Imaging Study of in vivo and ex vivo Biodistribution of Solid Lipid Nanoparticles/p. International Journal of Nanomedicine. 2020 Mar;Volume 15:1745–58.
[43] Fan W, Yu Z, Peng H, He H, Lu Y, Qi J, et al. Effect of particle size on the pharmacokinetics and biodistribution of parenteral nanoemulsions. International Journal of Pharmaceutics [Internet]. 2020;586:119551. Available from: https://www.sciencedirect.com/science/article/pii/S0378517320305354
[44] Busmann EF, Lucas H. Particle Engineering of Innovative Nanoemulsion Designs to Modify the Accumulation in Female Sex Organs by Particle Size and Surface Charge. Vol. 14, Pharmaceutics . 2022.
[45] Muthu MS, Wilson B. Challenges posed by the scale-up of nanomedicines. Nanomedicine [Internet]. 2012 Mar 1;7(3):307–9. Available from: https://doi.org/10.2217/nnm.12.3
[46] Choi SJ, McClements DJ. Nanoemulsions as delivery systems for lipophilic nutraceuticals: strategies for improving their formulation, stability, functionality and bioavailability. Food Science and Biotechnology [Internet]. 2020;29(2):149–68. Available from: https://doi.org/10.1007/s10068-019-00731-4

[47] Zhang Z, Huang J, Jiang S, Liu Z, Gu W, Yu H, et al. A high-drug-loading self-assembled nanoemulsion enhances the oral absorption of probucol in rats. Journal of Pharmaceutical Sciences [Internet]. 2013 Apr 1;102(4):1301–6. Available from: https://doi.org/10.1002/jps.23460

[48] Inal A, Yenipazar H, Şahin-Yeşilçubuk N. Preparation and characterization of nanoemulsions of curcumin and echium oil. Heliyon [Internet]. 2022 Feb 16;8(2):e08974–e08974. Available from: https://pubmed.ncbi.nlm.nih.gov/35243093

[49] Hirsjärvi S, Dufort S, Gravier J, Texier I, Yan Q, Bibette J, et al. Influence of size, surface coating and fine chemical composition on the in vitro reactivity and in vivo biodistribution of lipid nanocapsules versus lipid nanoemulsions in cancer models. Nanomedicine: Nanotechnology, Biology and Medicine [Internet]. 2013;9(3):375–87. Available from: https://www.sciencedirect.com/science/article/pii/S1549963412005199